Nanoscale Fe islands on MgO(001) produced by molecular-beam epitaxy

S. M. Jordan, R. Schad, A. M. Keen, M. Bischoff, D. S. Schmool,* and H. van Kempen†
Research Institute for Materials, University of Nijmegen, Toernooiveld 1, NL-6525 ED Nijmegen, The Netherlands
(Received 3 August 1998)

We report that a 10-nm thick Fe film grown at an elevated temperature on MgO(001) forms isolated islands of diameter between 10 and 100 nm. Increasing the deposition temperature causes the islands to decrease in diameter. The resulting films are electrically insulating but show electrical transport properties that vary strongly with growth temperature when capped with 2 nm Au. Films grown at a temperature of 743 K showed a giant magnetoresistance of 0.7% when measured at room temperature. [S0163-1829(99)01012-7]

I. INTRODUCTION

The magnetic and transport properties of granules of magnetic material suspended within a nonmagnetic metal matrix have received much interest on account of the discovery of the giant magnetoresistance (GMR) effect[1,2] in these granular systems.[3] This effect arises from spin-dependent scattering of electrons at the ferromagnet/normal-metal interface, and depends critically on the material's physical structure.[4] The physical mechanisms governing this effect are of fundamental importance. However, both measuring and controlling the properties of an inhomogeneous system are difficult, and few studies report the correlation of transport and structural properties.[5]

Here we report a method by which a granular system can be formed. When Fe is grown at temperatures above 700 K, a sharp transition occurs, resulting in the formation of discontinuous islands instead of the continuous films previously reported.[6,7] Their size distribution can be controlled simply by changing the deposition temperature, the islands becoming *smaller* as the temperature *increases*. The structure of the film can then be measured directly using a scanning probe microscope. Capping the film with Au allows electrical conduction to take place, with GMR occurring due to the presence of ferromagnet/normal-metal interfaces. This system can thus provide an unprecedented opportunity to correlate structural, magnetic, and transport properties.

II. SAMPLE PREPARATION

Commercially obtained substrates[8] were cleaned ultrasonically, first in acetone and then propan-2-ol to remove surface contamination. Atomic force microscopy (AFM) showed large terraces of atomic flatness extending over as much as 200 nm. After introduction into the molecular-beam-epitaxy (MBE) chamber they were heated by electron bombardment of the sample holder to 1300 K and held at that temperature for 1 min. This procedure is sufficient to desorb any adsorbed hydrogen.[9–11] After cooling, Auger-electron spectra (AES) were taken, which showed a KLL carbon peak equivalent to 6% of 1 monolayer.

Fe was then deposited from a Knudsen cell (temperature 1680 K) at a rate of 0.13 nm per minute, the rate being measured before growth by a quartz-crystal thickness meter. In all cases, 10 nm of Fe was deposited. The sample was held at the desired temperature to within 10 K throughout the deposition. The pressure during growth was 1×10^{-9} mbar or lower. After growth of the Fe layer, the sample was cooled to 370 K, and a 2-nm layer of Au was deposited. This thickness was felt to provide sufficient coverage to protect the Fe from oxidation without obscuring the structure of the iron. AES showed strong Au peaks, with slight Fe and O peaks visible.

III. SCANNING PROBE MICROSCOPE INVESTIGATION

We examined the completed Au covered films with both AFM and scanning tunneling microscopy (STM). The AFM measurements were made *ex situ* in the ''tapping mode'' using a commercial Si tip of radius 10 nm and internal angle 30°.[12] Micrographs are presented in Figs. 1 and 2 for growth temperatures of 793 and 953 K, respectively. Both AFM images have been ''flattened'' by subtracting each scan line's average slope.

The image of the sample grown at the lower temperature shows large (up to 100 nm major axis) islands of widely varying shapes and sizes. Channels of typically 2-nm depth can be observed between the islands, which possibly contain smaller islands that are not well resolved due to the curvature of the tip. At this temperature both AFM and STM give similar results.

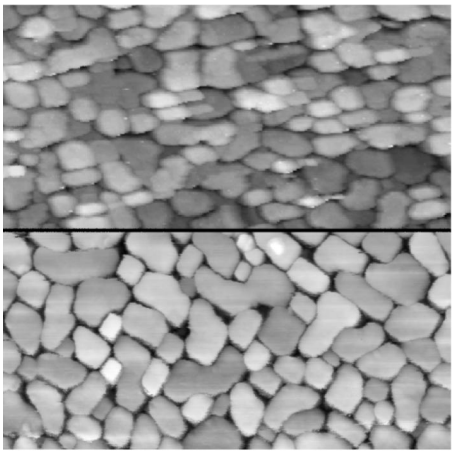

FIG. 1. STM (top) and AFM (bottom) micrograph of 10 nm Fe grown at 793 K. Black-white contrast approximately 20 nm. Images are 1000×500 nm.

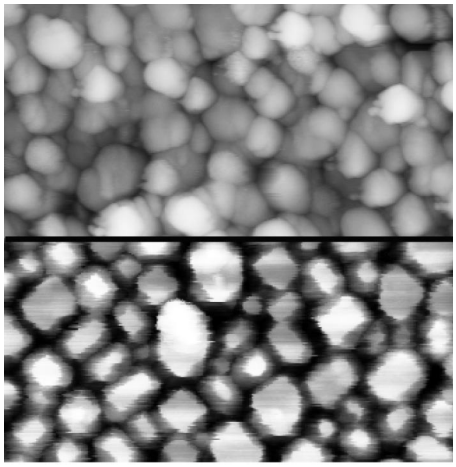

FIG. 2. STM (top) and AFM (bottom) micrograph of 10 nm Fe grown at 953 K. Black-white contrast approximately 30 nm. Images are 500×250 nm.

When the deposition temperature is increased to 953 K, the islands approximately halve in area, and the depth of the channels between them increases. The AFM and STM images are different here, the former showing pyramids instead of round islands. This is due to the convolution of the pyramidal AFM tip and the surface.[13] The STM has greater spatial resolution on account of tunneling occurring from a single atom on the tip, but the overall aspect ratio of our mechanically prepared Pt-Ir tips is unknown. STM is practically difficult on this system due to the rapid appearance of double tip effects; thus, we will base the analysis to follow on the AFM images.

Height profiles of two AFM images are shown in Fig. 3 with the tip profile superposed. At the higher growth temperature both the increased depth and greater steepness of the channels between the islands is clear. The true structure of the edges of the islands is not reflected by the height profiles, since the curvatures of the tip (radius 10 nm) and sample are comparable. The true steepness is the sum of the two curvatures, provided that the tip touches only one part of the sample at once.[14]

A property of great interest for correlation with physical properties is the average area of the islands. This was assessed in two ways. First, an estimate of the average island area A_c was measured by counting the number of islands

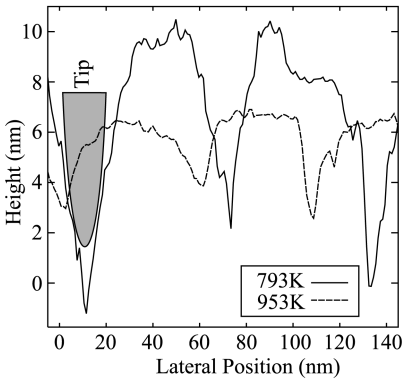

FIG. 3. Height profiles of the AFM images in Figs. 1 and 2. The tip profile (10-nm radius of curvature) is superposed.

TABLE I. Average island areas using two different measurements. The values A_c were found by counting the number of islands in a square image of reasonable size. The second and third columns used direct measurements of each island area. The figures in brackets represent the area converted into a radius (in nm). The resistivities of the completed samples are given. A value of ∞ indicates that the resistance was too great to measure with standard techniques.

Growth temp. (K)	A_c $(\text{nm})^2$	$\overline{A}$ $(\text{nm})^2$	σ (nm)	$\rho(\mu\Omega\,\text{cm})$
693		–continuous–		7.7
743	5900 (44)	3640 (34)	0.81	5.7×10^2
793	5600 (42)	3100 (31)	0.90	7.0×10^4
843	4900 (40)	3000 (31)	0.82	7.3×10^5
893	4400 (37)	2900 (30)	1.10	3.4×10^6
943	2200 (26)	1480 (22)	0.71	∞
993	1700 (23)	1150 (19)	0.96	∞

within a square image of sufficient size to contain approximately 600 islands. The average radius was then calculated using the formula

$$\overline{r}=\sqrt{\frac{A_c}{\pi}}, \tag{1}$$

which assumes each island to be circular and that the islands cover the surface with a packing fraction of 0.87. The second method was to trace the outline of each island manually and then measure the areas using commercial software. The radii were also calculated using Eq. (1). Table I gives the results. These two methods do give differing results, but they rely on different premises. The first assumes that each island is circular and ignores the fact that the spaces between the islands will be larger than that between perfect circles. The second relies on manual measurement and tends to underestimate the island areas. The actual value will be between the two numbers.

Figure 4 shows the histograms of island areas for two growth temperatures. Superposed is the log-normal distribution

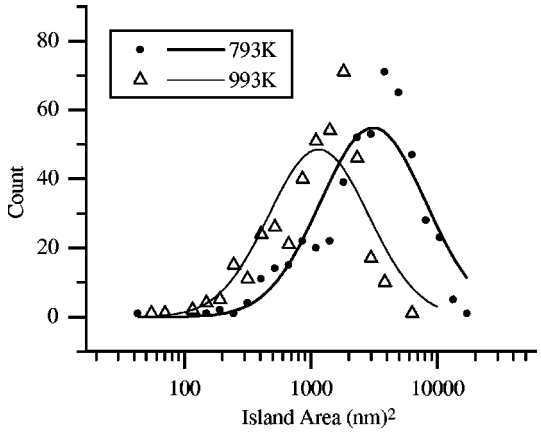

FIG. 4. Island area distribution for two different temperatures. The lines show the log-normal distribution for the means and standard deviations in Table I.

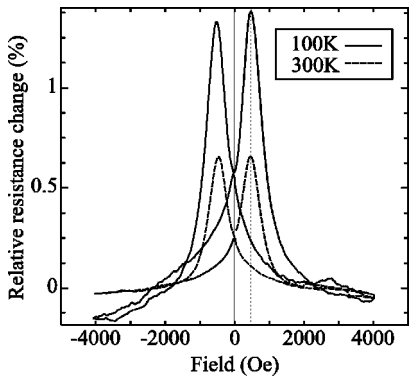

FIG. 5. Magnetoresistance curves with **H** and the current normal to each other, but both in the plane of the film.

$$N(A)=N_0\exp-\frac{[\ln(A/\overline{A})]^2}{2\sigma^2}. \tag{2}$$

This function has no physical significance,[15] however, it fits the experimental data reasonably well. The mean and standard deviation were found using

$$\ln\overline{A}=\sum_{n=0}^{N}\ln(A_n)/N \tag{3}$$

and

$$\sigma^2=\sum_{n=0}^{N}\ln(2A_n)/N-\left[\sum_{n=0}^{N}\ln(A)/N\right]^2. \tag{4}$$

These results show that the measured island area drops by a factor of 3 as the temperature increases by 250 K, but the overall distribution of sizes remains the same.

IV. ELECTRICAL TRANSPORT PROPERTIES

The electrical resisitivities of these films are not only much greater than that of a continuous film but depend very strongly on deposition temperature. Table I shows that an increase in ρ of almost two orders of magnitude of an island (743 K) over a continuous (693 K) film. Raising the growth temperature further causes ρ to increase still further until the film becomes essentially an insulator.

The resistivities of the samples grown at 793, 843, and 893 K all showed a negative temperature coefficient. All approximately followed the law

$$\rho=\rho_0\exp(\gamma/T^n), \tag{5}$$

suggested by Sheng,[16] with $n=0.5$. This gives approximately a factor of 10 decrease in ρ when the T is increased from 200 to 300 K. This temperature dependence indicates that the islands are electrically isolated and conduction occurs through thermally generated carriers.

Figure 5 shows the magnetoresistance of the sample grown at 743 K for two measurement temperatures with the measurement current and the applied field normal to each other but in the plane of the film. The same behavior is seen when the current and field are parallel. Reducing the temperature to 100 K approximately doubled the GMR ratio. This behavior occurs due to spin-dependent scattering at the Fe/Au interfaces. As the applied field increases, the magnetization vectors of the Fe become aligned, and less scattering occurs leading to a lower resistance. GMR may also occur in the films grown at higher temperature but this measurement is practically difficult due to the magnitude of ρ and the strong temperature dependence.

If we assume that maximum resistance occurs at zero net magnetization,[17] then Fig. 5 gives the coercivity of our sample as 500 Oe. It is also clear that the saturation field of the sample is high: the resistivity is still changing as **H** increases above 10 kOe. Kreuzer *et al.*[18] report that system of Fe ''dots'' 50 nm in diameter and periodicity 320 nm clearly saturates at a field of 1 kOe.

Wang and Xiao *et al.*[19] have studied the temperature dependence of the GMR effect in the $Co_{20}Ag_{80}$ granular system. They found that reducing the temperature from 300 to 100 K increased the magnetoresistance ratio by 50%. They claim that this change is due to a reduced magnetization at finite temperature due to spin-wave excitations. However, they also found a change in the *form* of the field dependence of the resistance, indicating that the magnetic properties of the sample change strongly with temperature. Our results do not show any change in the form of the field dependence.

V. DISCUSSION

We can only explain the rapid change in ρ with growth temperature as a change in the properties of the Au/Fe interface. The geometry of the Fe islands does not change sufficiently to cause an increase of this order; thus the steepening sides of the islands must prevent the Au from making contact. Au and Fe are immiscible, and the angle between the substrate and the Fe may make a difference to the surface tension required to connect the two. The Au atoms were incident at an angle of 15° to the normal during deposition, and since the slope of the sides of the islands is comparable to this (Fig. 3), shadowing may play a role. A thicker Au layer should lower ρ and allow a direct correlation to be made between the magnetoresistance behavior and the distribution of island sizes. A possibility to tailor GMR properties in a simple way is also very valuable.

We have yet to explain why islands form; any theory must support not only the existence of the transition between islanded and continuous films at 700 K, but the fact that the islands become smaller with increasing temperature. Several authors[7,20,21] have studied islanded Fe films on MgO, but at coverages in the monolayer regime. It also may be possible that many other metal/insulator systems have this behavior if the deposition temperature is sufficient.

ACKNOWLEDGMENTS

This work has been financially supported by the Dutch Foundation for the Fundamental Research of Matter (FOM), which is, in turn, financially supported by the Dutch Organization for Scientific Research (NWO). R.S. would like to acknowledge the assistance of the Brite-Euram program of the European Community (Contract No. BRE 2-CT93-0569). D.S.S. was funded by the TMR program of the European Union.

*Present address: Laboratoire de Magnétisme et d'Optique, Université de Versailles-Saint Quentin – CNRS, Bâtiment Fermat, 45 Avenue des Etats-Unis, 78035 Versailles, France.
†Corresponding author. FAX: 3652190. Electronic address: hvk@sci.kun.nl

[1] G. Binasch, P. Grünberg, F. Saurenbach, and W. Zinn, Phys. Rev. B **39**, 4828 (1989).
[2] M.N. Baibich *et al.*, Phys. Rev. Lett. **61**, 2472 (1988).
[3] S.S.P. Parkin, R.F.C. Farrow, T.A. Rabedeau, R.F. Marks, G.R. Harp, Q. Lam, C. Chappert, M.F. Toney, R. Savoy, and R. Geiss, Europhys. Lett. **22**, 455 (1993).
[4] B. Dieny, S.R. Teixeira, B. Rodmacq, C. Cowache, S. Auffret, O. Redon, and J. Pierre, J. Magn. Magn. Mater. **130**, 197 (1994).
[5] K. Ounadjela, S.M. Thompson, J.F. Gregg, A. Azizi, M. Gester, and J.P. Deville, Phys. Rev. B **54**, 12 252 (1996).
[6] S.M. Jordan, J.F. Lawler, R. Schad, and H. van Kempen, J. Appl. Phys. (to be published).
[7] B.M. Lairson, A.P. Payne, S. Brennan, N.M. Rensing, B.J. Daniels, and B.M. Clemens, J. Appl. Phys. **78**, 4449 (1995).
[8] Crystal GmbH, Ostendstrasse 2-14, 12459 Berlin, Germany.
[9] M.J. Stirniman, C. Huang, R.S. Smith, S.A. Joyce, and B.D. Kay, J. Chem. Phys. **105**, 1295 (1996).
[10] M.A. Karolewski and R.G. Cavell, Surf. Sci. **271**, 128 (1992).
[11] O. Robach, G. Renaud, and A. Barbier, Surf. Sci. **401**, 227 (1998).
[12] Digital Instruments Inc., 520 E. Montecito St., CA 93103.
[13] F. Atamny and A. Baiker, Surf. Sci. **323**, L314 (1995).
[14] D. Keller, Surf. Sci. **253**, 353 (1991).
[15] J.A. Blackman, B.L. Evans, and A.I. Maaroof, Phys. Rev. B **49**, 13 863 (1994).
[16] P. Sheng, in *Electrical Transport and Optical Properties of Inhomogeneous Media*, edited by J.C. Garland and D.B.Tanner, AIP Conf. Proc. 40 (AIP, New York, 1978), Chap. II, pp. 143–153.
[17] J.Q. Xiao, J.S. Jiang, and C.L. Chien, Phys. Rev. Lett. **68**, 3749 (1992).
[18] S. Kreuzer, K. Prügl, G. Bayreuther, and D. Weiss, Thin Solid Films **318**, 219 (1998).
[19] J.Q. Wang and G. Xiao, Phys. Rev. B **50**, 3423 (1994).
[20] Y. Park, S. Adenwalla, G.P. Felcher, and S.D. Bader, Phys. Rev. B **52**, 12 779 (1995).
[21] C. Liu, Y. Park, and S.D. Bader, J. Magn. Magn. Mater. **111**, L225 (1992).